Diacylglycerol kinase δ regulates protein kinase C and epidermal growth factor receptor signaling

Tracy Crotty*, Jinjin Cai*, Fumio Sakane*†, Akinobu Taketomi*‡, Stephen M. Prescott*§¶, and Matthew K. Topham*§‖

*Huntsman Cancer Institute and §Department of Internal Medicine, University of Utah, 2000 Circle of Hope, Salt Lake City, UT 84112

Edited by Philip W. Majerus, Washington University School of Medicine, St. Louis, MO, and approved August 24, 2006 (received for review May 17, 2006)

Diacylglycerol kinases (DGKs) phosphorylate diacylglycerol (DAG) to terminate its signaling. To study DGKδ, we disrupted its gene in mice and found that DGKδ deficiency reduced EGF receptor (EGFR) protein expression and activity. Similar to EGFR knockout mice, DGKδ-deficient pups were born with open eyelids and died shortly after birth. PKCs are activated by DAG and phosphorylate EGFR to reduce its expression and activity. We found DAG accumulation, increased threonine phosphorylation of EGFR, enhanced phosphorylation of other PKC substrates, and increased PKC autophosphorylation in DGKδ knockout cells, indicating that DGKδ regulates EGFR by modulating PKC signaling.

Diacylglycerol kinases (DGKs) catalyze the phosphorylation of diacylglycerol (DAG) to produce phosphatidic acid (1, 2). DAG, the substrate of the DGK reaction, is a key intracellular signaling factor that activates PKCs, Ras guanyl nucleotide-releasing proteins, and some transient receptor potential channels (3, 4). DAG also recruits a number of proteins to membrane compartments, including the chimaerins, PKD, and the Munc13 proteins (3). Its effects on numerous and diverse targets underscores the importance of DAG signaling and indicates that DAG affects a broad array of signaling events. Because the consumption of DAG by DGKs is thought to attenuate these actions, the DGK reaction is biologically important and likely regulates numerous DAG signaling pathways.

Mammalian DGKs differ in their structures, patterns of tissue expression, and catalytic properties. Ten of them have been identified and are classified into five subtypes based on their structural motifs (1, 2, 5, 6). Their structural diversity and distinct expression patterns indicate that each isoform may perform a different biological function. Supporting functional diversity, the DGK knockout mice that have been studied to date have distinct phenotypes, including resistance to seizures in DGKε knockout mice (7), attenuated Ras signaling in DGKι knockouts (8), and hyperactive T cell signaling in DGKζ-deficient mice (9).

As a type II DGK, DGKδ has a characteristic pleckstrin homology domain and a sterile α-motif domain (Fig. 1*A*). To determine its biological function, we generated mice with a targeted mutation of the DGKδ gene. Our data indicate an important role for DGKδ in modulating PKC and EGF receptor (EGFR) signaling.

Results and Discussion

We used mice to make a targeted deletion of the N-terminal portion of the DGKδ catalytic domain (see Fig. 7, which is published as supporting information on the PNAS web site). Southern blot analysis of tail DNA confirmed proper insertion of the targeting vector (data not shown), and RT-PCR demonstrated absence of DGKδ mRNA in homozygous mutant cells (Fig. 7*C*). Also confirming DGKδ gene inactivation, DGKδ protein was absent in knockout keratinocyte and dermal fibroblast cell lysates (Fig. 7*D*). Deleting DGKδ did not significantly affect mRNA expression of other DGKs in brain tissue (Fig. 7*E*). Finally, to establish the expression pattern of DGKδ in WT mice, we performed RT-PCR using mouse tissues and found DGKδ mRNA in most tissues and in developing embryos (Fig. 7*F*).

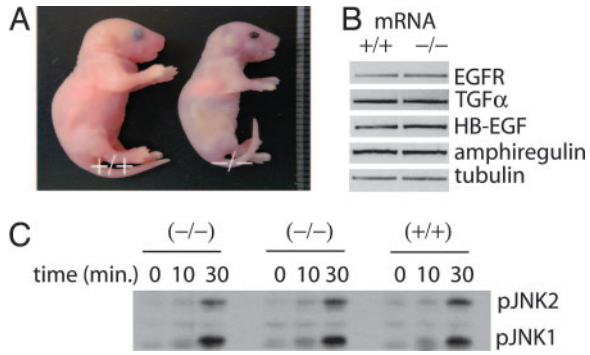

Fig. 1. Morphology of DGKδ-deficient mice, expression of EGFR and its growth factors, and JNK signaling. (*A*) Newborn DGKδ knockout mice had open eyelids and were smaller than normal littermates. (*B*) Using mRNA from primary keratinocytes, we detected EGFR, TGFα, HB-EGF, amphiregulin, and tubulin by RT-PCR. (*C*) DGKδ mutant or WT immortalized embryo fibroblasts were treated with activin B (10 ng/ml) for the indicated times, and phosphorylated JNK1 and JNK2 (pJNK1 and 2) were detected by immunoblotting.

Heterozygous mice ($dgkd^{+/-}$) were viable and fertile, and the genotypes of newborn progeny from $dgkd^{+/-}$ intercrosses were consistent with Mendelian inheritance. Unexpectedly, the homozygous null defect was invariably lethal: $dgkd^{-/-}$ mice developed respiratory difficulty and died within 24 h after birth. Additionally, most $dgkd^{-/-}$ fetuses were smaller than WT and heterozygous littermates: Newborn $dgkd^{-/-}$ mice weighed 1.10 ± 0.21 g ($n = 11$), whereas WT mice weighed 1.39 ± 0.15 g ($n = 11$). Newborn $dgkd^{-/-}$ mice were identifiable by their open eyelids (Fig. 1*A*). Normally, eyelids fuse at approximately embryonic day (E) 16.5 and do not open until approximately postnatal day 14. In contrast, at E17.5 and at birth, all $dgkd^{-/-}$ fetuses that we examined had open eyelids.

Several genetic abnormalities result in the phenotype of open eyelids at birth. In most cases, these mutations have disrupted EGFR signaling. For example, disrupting the genes encoding c-Jun (10, 11), JNK (12), or MEK (MAPK/ERK kinase) kinase 1 (13) resulted in reduced expression of EGFR and/or its growth

Author contributions: T.C., J.C., F.S., A.T., S.M.P., and M.K.T. designed research; T.C., J.C., F.S., A.T., and M.K.T. performed research; T.C., J.C., and M.K.T. analyzed data; and M.K.T. wrote the paper.

The authors declare no conflict of interest.

This article is a PNAS direct submission.

Abbreviations: DAG, diacylglycerol; DGK, DAG kinase; EGFR, EGF receptor; TACE, TNFα converting enzyme; HB-EGF, heparin binding EGF; cnPKCs, conventional and novel PKCs; pT EGFR, threonine-phosphorylated EGFR; pY EGFR, phospho-tyrosine EGFR; MARCKS, myristoylated alanine-rich C kinase substrate.

†Present address: Department of Biochemistry, Sapporo Medical University School of Medicine, Sapporo 060-8556, Japan.

‡Present address: Department of Surgery, Kyushu University, Fukuoka 812-8582, Japan.

¶Present address: Oklahoma Medical Research Foundation, 825 Northeast 13th Street, Oklahoma City, OK 73104.

‖To whom correspondence should be addressed. E-mail: matt.topham@hci.utah.edu.

factor ligands, causing an open-eyelid phenotype. And disrupting TNFα converting enzyme (TACE), which proteolytically releases EGFR ligands from the cell surface, or EGFR itself similarly caused an open-eyelid phenotype (14–16). TACE is predominantly responsible for shedding the six known EGFR ligands (17). We found no differences in $dgkd^{-/-}$ and WT embryo fibroblasts in TACE expression or in their ability to shed overexpressed TGFα, heparin binding EGF (HB-EGF), amphiregulin, and betacellulin (data not shown). Nor were there differences in TNFα or p75 TNFα receptor shedding in newborn $dgkd^{-/-}$ and $dgkd^{+/+}$ liver homogenates (data not shown). Based on these results, we concluded that DGKδ did not regulate TACE activity.

Several mutations that interrupted the JNK signaling pathway reduced mRNA expression of EGFR and/or its growth factors and resulted in the open-eyelids-at-birth phenotype (10–13). Using semiquantitative RT-PCR, we tested expression of mRNA encoding EGFR, HB-EGF, TGFα, and amphiregulin in primary keratinocytes isolated from either WT or DGKδ-null mice and found similar expression of EGFR and growth factor mRNA in knockout cells compared with WT cells (Fig. 1*B*). We also found identical phosphorylation of JNK1/2 in $dgkd^{-/-}$ and $dgkd^{+/+}$ embryo fibroblasts treated with activin B (Fig. 1*C*). Thus, deleting DGKδ did not affect JNK signaling pathways known to cause aberrant mRNA expression of EGFR or its growth factors.

Next, we examined EGFR protein in primary keratinocytes and consistently found reduced EGFR expression in DGKδ-null keratinocytes (Fig. 2 *A* and *B*). To verify reduced EGFR expression, we immunostained EGFR in paraffin sections from $dgkd^{-/-}$ or $dgkd^{+/-}$ newborn mice and found reduced levels of EGFR in all layers of the epidermis in $dgkd^{-/-}$ mice. EGFR was most significantly reduced in the basal layer of the epidermis (Fig. 2*C*). These data indicated that DGKδ is necessary for proper expression of EGFR protein. To verify that reduced DGKδ attenuated EGFR protein expression, we used RNAi to knock down DGKδ in SCC-9 cells, a squamous cell cancer line. Consistent with reduced EGFR expression in DGKδ-deficient mice, we found significantly reduced EGFR protein in DGKδ knockdown cells (Fig. 2 *D* and *E*).

Our data indicated a crucial role for DGKδ in maintaining EGFR protein expression. We considered the possibility that DGKδ might maintain this expression by regulating DAG signaling. PKC enzymes are major targets of DAG and are known to phosphorylate human EGFR at threonine-654 (T654) (18, 19). The consequences of this phosphorylation are twofold. First, it reduces EGFR tyrosine kinase activity by an unknown mechanism (18–20). Second, it induces internalization of EGFR but then causes the silenced receptor to be recycled to the plasma membrane (21–24). Combined, the overall immediate effect of PKC phosphorylation is to blunt EGFR signaling. The negative effects on EGFR are further augmented if PKC activation continues for several hours, at which point, EGFR is degraded, and its levels fall (25).

By consuming DAG, DGKs can reduce PKC activity (26–28), so we reasoned that deleting DGKδ might have increased PKC activity and caused excess T654 EGFR phosphorylation. To explore this possibility, we immunoprecipitated EGFR from newborn mouse brain lysates and then immunoblotted to detect phospho-Thr-X-Arg. In $dgkd^{-/-}$ mice, we found increased phospho-threonine EGFR compared with $dgkd^{-/-}$ and WT mice (Fig. 3*A* and *B*), which suggested that deleting DGKδ activated PKCs that then phosphorylated EGFR. To test whether expressing DGKδ could attenuate EGFR threonine phosphorylation, we expressed DGKδ1 in embryo fibroblasts, treated the cells with TGFα, and then immunoprecipitated EGFR and measured its threonine phosphorylation by Western blotting. We found that expressing DGKδ1 reduced the phosphorylation of T654 in

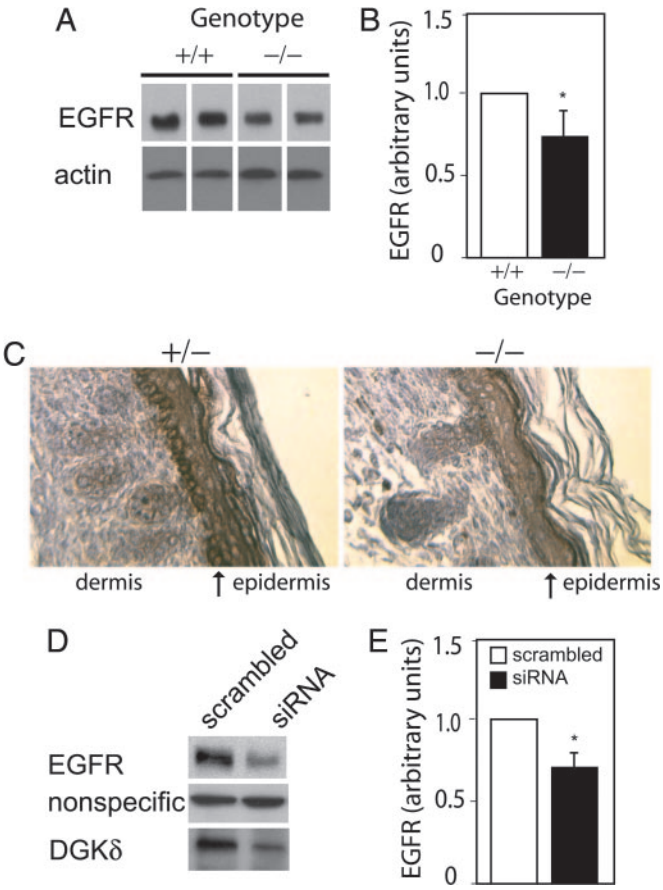

Fig. 2. DGKδ deficiency reduces EGFR expression. (*A*) EGFR and β-actin protein expression in WT or DGKδ knockout primary keratinocytes was detected by Western blotting. Samples from two WT and two knockout lysates are shown; lane separations were removed from the blot for clarity. (*B*) Scanning densitometry of EGFR Western blots demonstrated significant reduction of EGFR expression in DGKδ-null cells. Shown are mean values and SD for DGKδ knockout mice compared with WT (*, $P < 0.02$; $n = 12$). (*C*) Back skin from heterozygous (+/−) and homozygous (−/−) DGKδ mutant mice was immunostained to detect EGFR (brown) and counterstained with hematoxylin. The arrows mark the basal layer of the epidermis. (*D*) Using siRNA, DGKδ was knocked down in SCC-9 cells. After 48 h, EGFR and DGKδ were detected by immunoblotting. Shown is a nonspecific band detected by the anti-EGFR antibody that did not change upon knockdown of DGKδ. There was also no change in expression of β-actin (not shown). (*E*) Scanning densitometry of Western blots from six experiments demonstrated that knockdown of DGKδ reduced EGFR expression. Shown are mean values and SD of DGKδ siRNA compared with scrambled control siRNA (*, $P < 0.05$).

EGFR (Fig. 3 *C* and *D*). Together, our data indicate that DGKδ regulates PKCs that phosphorylate EGFR.

Increased T654 EGFR phosphorylation in $dgkd^{-/-}$ mice would be expected to eventually reduce EGFR protein expression levels by causing its degradation. To test whether we could rescue EGFR expression by inhibiting PKCs, we treated $dgkd^{-/-}$ keratinocytes with a broad-spectrum PKC inhibitor, bisindolylmaleimide I, for 1 h and found partial rescue of EGFR expression in the cells (Fig. 3*E*). Other PKC inhibitors, Gö6976 and Gö6983, also increased EGFR expression in $dgkd^{-/-}$ keratinocytes and SCC-9 cells treated with DGKδ siRNA (data not shown). Because SCC-9 cells and keratinocytes express at least five PKC isoforms and the inhibitors that we used would not affect all of them, it was not surprising that the inhibitors did not fully restore EGFR expression. Because PKCs participate in endosome formation and trafficking (29, 30) and can phosphorylate and regulate dynamin (31), we explored the possibility that

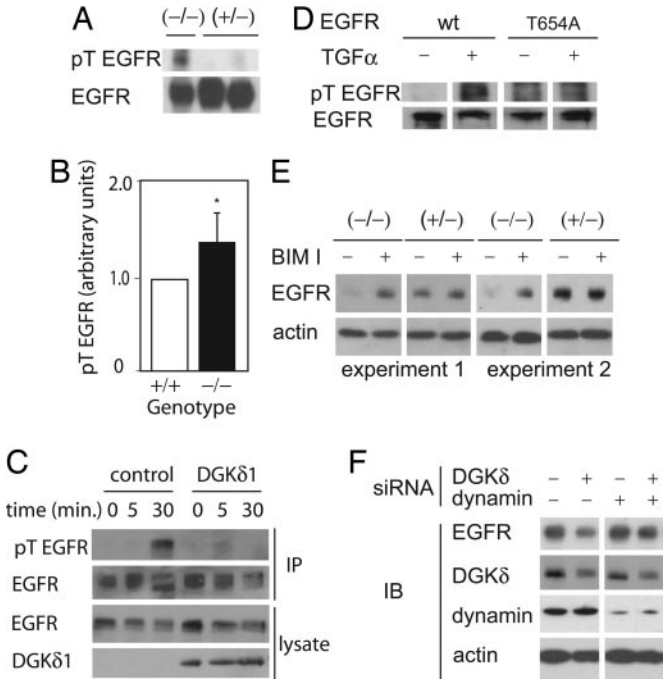

Fig. 3. DGKδ regulates threonine phosphorylation of EGFR. (*A*) EGFR was immunoprecipitated from brain lysates of newborn heterozygous or DGKδ mutant mice. The amount of threonine-phosphorylated EGFR (pT EGFR) was detected by immunoblotting by using a phospho-Thr-X-Arg antibody. The membrane was stripped and reprobed to detect total EGFR. (*B*) Scanning densitometry from five experiments demonstrated increased pT EGFR in tissues from DGKδ-deficient mice compared with WT mice. Shown are mean values and SD (*, $P < 0.05$). (*C*) Immortalized embryo fibroblasts were transfected with EGFR and either a control vector or DGKδ1. Starved cells were treated for the indicated times with TGFα (10 ng/ml), and EGFR was immunoprecipitated. After detecting pT EGFR by immunoblotting, the membrane was stripped and reprobed to detect total EGFR. Cell lysates were probed to detect either EGFR or DGKδ1. (*D*) Embryo fibroblasts were transfected with either WT or a T654A EGFR mutant. Starved cells were treated for 10 min with or without TGFα (20 ng/ml) and lysed. EGFR was precipitated, followed by detection of pT EGFR by Western blotting. The blot was stripped and reprobed to detect total EGFR in the precipitates. (*E*) DGKδ-deficient or heterozygous primary keratinocytes were starved and then treated for 1 h with or without bisindolylmaleimide I (200 nM). EGFR and actin were detected by Western blotting. Similar results were obtained with the PKC inhibitors Gö6976 and Gö6983 (100 nM). (*F*) SCC-9 cells were transfected with siRNA duplexes for DGKδ and/or dynamin II. At 24 h, EGFR, DGKδ, dynamin II, and β-actin were detected in cell lysates by immunoblotting.

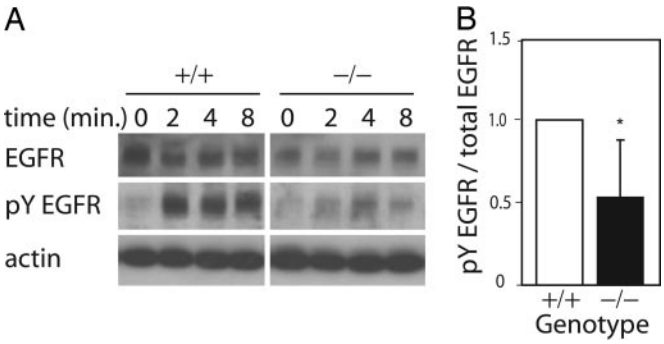

Fig. 4. Reduced EGFR kinase activity in DGKδ-deficient cells. (*A*) Primary mouse keratinocytes were starved and treated with TGFα (5 ng/ml) for the indicated times. EGFR, pY EGFR, and β-actin were detected by immunoblotting. (*B*) Western blots of pY EGFR from cells treated with TGFα were quantified by scanning densitometry. Values were normalized to total EGFR (no TGFα treatment). There was a significant reduction in normalized pY EGFR in DGKδ-null cells compared with WT cells. Shown are mean values and SD (*, $P < 0.02$; $n = 6$).

the effects on EGFR might be due to its endocytosis and degradation. By using siRNA to reduce expression of both DGKδ and dynamin II, we found that dynamin knockdown partly rescued EGFR expression (Fig. 3*F*). Together, our data indicate that the reduced EGFR expression in DGKδ-deficient cells requires PKC activity and functional endocytosis.

Because T654 EGFR phosphorylation also affects EGFR kinase activity, we next examined the effects of deleting DGKδ on EGFR kinase activity by treating primary keratinocytes with TGFα and then measuring phospho-tyrosine EGFR (pY EGFR). We found significantly reduced EGFR autophosphorylation in DGKδ-deficient cells (Fig. 4*A*), indicating that the absence of DGKδ attenuated EGFR activity. To quantify the effect of deleting DGKδ on EGFR kinase activity, we used scanning densitometry to normalize pY EGFR to total EGFR expression and found a significant reduction of phospho-EGFR in DGKδ knockout keratinocytes (Fig. 4*B*). Together, our results indicate that deleting DGKδ increases PKC activity, causing threonine phosphorylation of EGFR. This, in turn, marks EGFR for degradation and decreases its intrinsic tyrosine kinase activity.

The effect of DGKδ on PKC activity suggested that DGKδ negatively regulates DAG signaling. To determine whether deleting DGKδ affected DAG levels, we assayed the amount of DAG in immortalized embryo fibroblasts and found significantly more DAG in $dgkd^{-/-}$ cells compared with $dgkd^{+/+}$ cells, both in basal and growth factor-stimulated states (Fig. 5*A*). Together, these data suggested that DGKδ reduces DAG levels and consequently inhibits PKC activity. DGKs regulate specific signaling events through their interactions with DAG-activated proteins such as the PKCs (8, 26, 32, 33). There are two splice variants of DGKδ; to test whether either of them could bind PKCs, we coexpressed each splice variant with each of the DAG-activated PKC isotypes (α, δ, ε, and η) found in keratinocytes and then immunoprecipitated the DGK. By immunoblotting, we found that both DGKδ splice variants coimmunoprecipitated each PKC isotype that we tested (Fig. 5*B*). Thus, DGKδ potentially binds and regulates multiple PKC isotypes.

The open eyes at birth and respiratory distress in newborn mutant mice suggested that DGKδ has an important role in lung and keratinocyte function. Supporting this possibility, we detected expression of DGKδ in mouse lung and keratinocytes by RT-PCR and protein blotting (Fig. 7 *D* and *F*). To determine whether PKC activity correlated with expression of DGKδ in these tissues, we immunostained lung sections from newborn mice by using an antibody that recognized phospho-Thr-X-Arg, a common PKC substrate. There was strong immunostaining in the epithelium of the large airways in $dgkd^{-/-}$ mice compared with $dgkd^{+/-}$ mice (Fig. 5*C*), which corresponded to the region of DGKδ mRNA expression detected by *in situ* analysis (Fig. 5*C*). In the skin of $dgkd^{-/-}$ mice, we found increased phospho-Thr-X-Arg immunostaining throughout the dermis and epidermis, whereas in $dgkd^{+/-}$ skin, immunostaining was limited to the epidermis (Fig. 5*D*). The changes in phospho-Thr-X-Arg were consistent with expression of DGKδ in primary dermal fibroblasts and keratinocytes (Fig. 7*D*). Keratin 6 protein is upregulated by phorbol esters, which activate conventional and novel PKCs (cnPKCs) (34). We examined expression of keratin 6 as an additional assessment of PKC activity in the mice and found that it was highly expressed in the epidermis of DGKδ-null mice and extended into the dermis and muscle (Fig. 5*D*). In $dgkd^{+/-}$ mice, keratin 6 expression was confined to the epidermis and hair follicles (Fig. 5*D*). The increased phospho-Thr-X-Arg

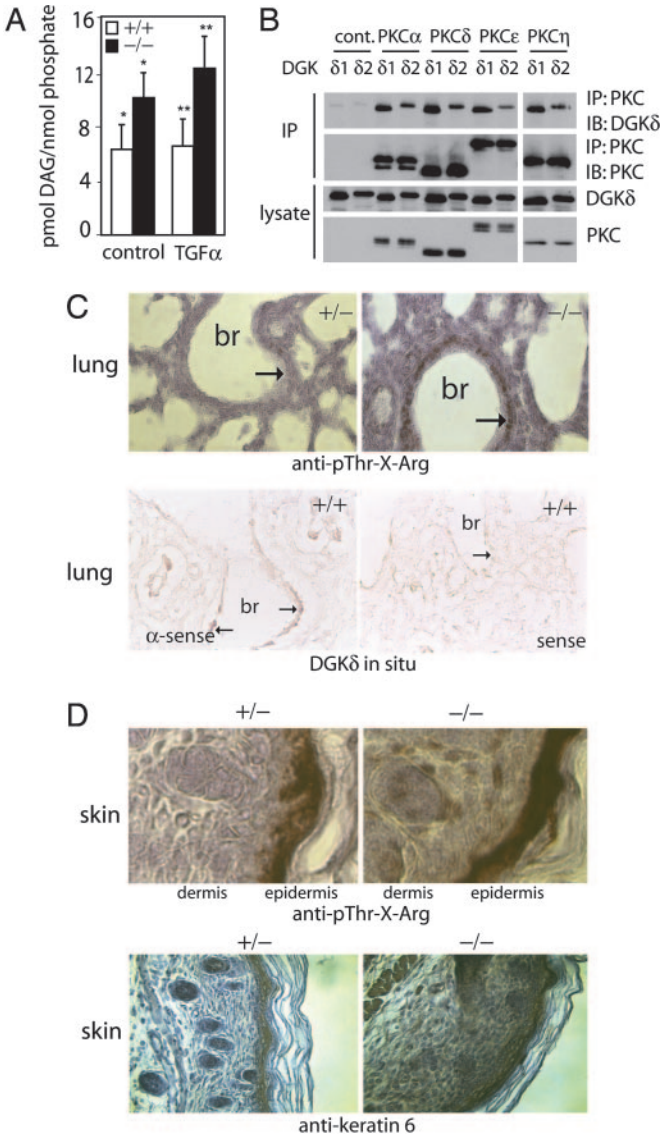

Fig. 5. DAG levels and assessment of PKC activity. (*A*) DAG quantity in starved or TGFα-treated (10 ng/ml for 15 min), immortalized embryo fibroblasts was normalized to lipid phosphate. Shown are mean values and SD ($n = 4$). * and ** indicate that the changes were significant ($P < 0.05$) as calculated by one-tailed *t* tests. (*B*) FLAG-DGKδ1 or FLAG-DGKδ2 was cotransfected into MCF-7 cells with either control vector or a PKC isotype with a Myc epitope tag. The PKC was immunoprecipitated with anti-Myc antibodies, and coimmunoprecipitation of DGKδ was detected by immunoblotting using anti-FLAG antibodies. (*C Upper*) Sections from heterozygous (+/−) or DGKδ-null (−/−) newborn mouse lung that were immunostained to detect phospho-Thr-X-Arg and counterstained with hematoxylin. In *dgkd*$^{-/-}$ mice, there was increased immunostaining (brown, marked by arrows) in the epithelial lining of the major bronchi (br). (*C Lower*) Lung sections from WT mice processed for *in situ* hybridization by using an antisense (α-sense) probe. Expression of DGKδ mRNA (brown, marked by arrows) in the epithelium of major bronchi is shown. There was minimal *in situ* staining of the epithelium (marked by arrow) with the sense probe. (*D*) Sections from heterozygous (+/−) or DGKδ-null (−/−) newborn mouse back skin immunostained brown to detect phospho-Thr-X-Arg or keratin 6 and counterstained with hematoxylin.

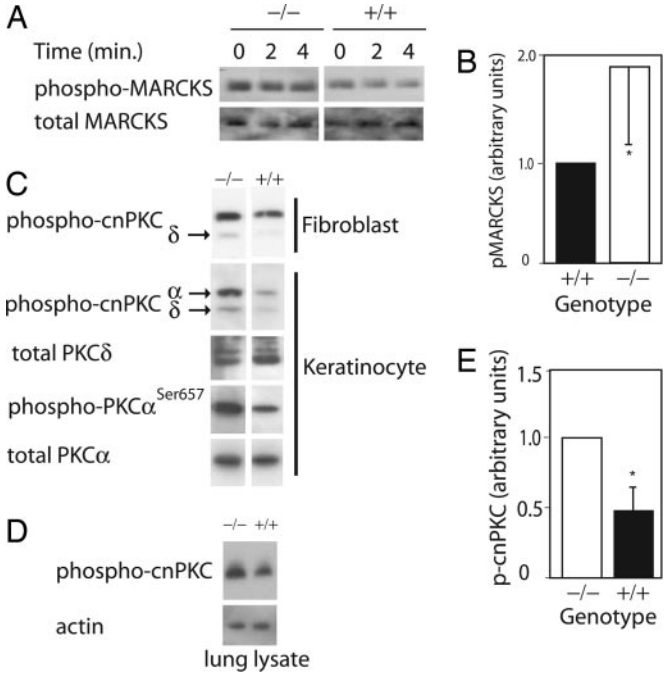

Fig. 6. Indicators of active PKCs. (*A*) Primary dermal fibroblasts were treated with TGFα (10 ng/ml) for the indicated times. Phospho-MARCKS was then detected in the cell lysates by immunoblotting. Membranes were stripped and reprobed to detect total MARCKS. (*B*) Western blots of phospho-MARCKS (pMARCKS) were quantified by scanning densitometry. There was a significant increase in pMARCKS in DGKδ-null cells compared with WT cells. Shown are mean values and SD from four experiments (*, $P < 0.05$). (*C*) Starved primary dermal fibroblast or keratinocyte lysates were immunoblotted to detect hydrophobic motif phosphorylation of cnPKCs (phospho-cnPKC) or phospho-PKCα$^{Ser\text{-}657}$. Blots were stripped and reprobed to detect total PKCα and PKCδ. Bands corresponding to PKCs α and δ are marked by arrows. (*D*) Lung lysates from DGKδ mutant or WT mice were immunoblotted to detect hydrophobic motif phosphorylation of cnPKCs (phospho-cnPKC). The blot was reprobed to detect β-actin. (*E*) Western blots of phospho-cnPKC (p-cnPKC) were quantified by scanning densitometry. There was a significant increase in cnPKC phosphorylation in DGKδ-null lung lysates compared with WT cells. Shown are mean values and SD (*, $P < 0.05$; $n = 3$).

and keratin 6 immunostaining in *dgkd*$^{-/-}$ mice indicated that deleting DGKδ led to increased PKC activity.

To confirm high levels of PKC activity in cells and tissue from the mice, we immunoblotted primary dermal fibroblast lysates to detect phospho-MARCKS (myristoylated alanine-rich C kinase substrate), a major substrate of PKCs, and found increased MARCKS phosphorylation in *dgkd*$^{-/-}$ cells compared with *dgkd*$^{+/+}$ cells (Fig. 6 *A* and *B*). Finally, to assess the abundance of active PKCs, we measured the levels of phospho-PKC in the lysates by immunoblotting with an antibody to detect hydrophobic motif serine/threonine phosphorylation of cnPKCs. We found that, in starved cells, there were at least two highly phosphorylated PKC isotypes in *dgkd*$^{-/-}$ cells compared with *dgkd*$^{+/+}$ cells. Using an antibody that is specific for phospho-PKCα$^{Ser\text{-}657}$, we determined that it was one of the highly phosphorylated PKCs in keratinocytes (Fig. 6*C*). Using scanning densitometry of Western blots, we found 1.20 (±0.04; $n = 5$; $P < 0.05$) times more phospho-PKCα in DGKδ-null keratinocytes compared with WT or heterozygous cells. And based on the mobility of PKCδ, which migrates farther than other PKCs, we determined that it was often phosphorylated at higher levels in *dgkd*$^{-/-}$ fibroblast and keratinocyte lysates (Fig. 6*C*). In five experiments using scanning densitometry, we found 1.63 (±0.95) times more phospho-PKCδ in DGKδ-null keratinocytes compared with WT or heterozygous cells. The changes in PKCδ were not statistically significant, likely because its phosphorylation was often, but not always, elevated in the knockout cells. To verify these observations in newborn mice, we immunoblotted newborn lung lysates and similarly found significantly increased phospho-cnPKC in *dgkd*$^{-/-}$ mice (Fig. 6 *D* and *E*). The lung

phospho-cnPKC band and the major phospho-cnPKC band in *dgkd*$^{-/-}$ fibroblast lysates did not correspond with PKCs α or δ, indicating that other PKC isotypes were highly phosphorylated in these cells.

We have shown that DGKδ is an important regulator of PKC activity and consequently modulates the phosphorylation of several PKC targets. Important among these targets is EGFR, whose expression and activity is reduced in DGKδ-deficient mice. But, in addition to its effects on EGFR, deleting DGKδ also affected other targets downstream of PKCs, including MARCKS and keratin 6, suggesting that aberrant phosphorylation of multiple PKC targets likely contributed to the phenotype of the mice. Supporting a role for DGKδ in regulating numerous PKC signaling events, other researchers have found that the DGKδ heterozygous mice developed insulin resistance and obesity (A. V. Chibalin, J. R. Zierath, personal communication). They found that DGKδ regulated insulin signaling in part by modulating PKC phosphorylation of IRS1 (insulin receptor substrate 1). Thus, it appears that DGKδ regulates PKCs and consequently modulates EGFR and insulin signaling. It is important to note, however, that DAG affects numerous proteins in addition to cnPKCs (35) and that DGKs regulate some of these DAG targets (8, 32, 33). So some of the effects caused by deleting DGKδ might also be mediated through non-PKC DAG targets, a possibility that will be important to explore.

Materials and Methods

Generation of Chimeric and Heterozygous Mice. We isolated, mapped, and subcloned three genomic clones spanning a total of >100 kb of the murine DGKδ gene. Exons 6–8 were replaced with a neomycin resistance cassette, and the fragment was cloned into the vector TK1-TK2A (provided by Kirk Thomas, University of Utah). Culture, selection of embryo stem cells, and screening of targeted clones were performed as described in ref. 8. Clones were screened by Southern blot analysis of EcoRI-digested genomic DNA probed with a 0.5-kb PCR fragment from the 3′ external region of the targeting vector (Fig. 7*B*). Two of 144 clones were identified as homologous recombinants. Homologous recombinant clones were injected into blastocysts of C57BL/6J mice and transferred into uteri of pseudopregnant C57BL/6J females. The resulting chimaeric animals were backcrossed to C57BL/6J mice, and heterozygous mutants were identified by Southern blot analysis of genomic tail DNA.

Southern Blot Analysis and RT-PCR. Genomic DNA (10 μg) digested with EcoRI (Fermentas, Bulington, ON, Canada) was subjected to agarose gel electrophoresis. Southern hybridization was performed as described in ref. 36 with a digitonin-labeled 3′ external probe (Roche Molecular Biochemicals, Indianapolis, IN).

Total RNA was prepared from primary embryo fibroblasts or primary keratinocytes by using TRIzol reagent (Invitrogen, Carlsbad, CA) and reverse-transcribed as described in ref. 37. The mouse multitissue cDNA panel was from Clontech (Mountain View, CA). RT-PCR using 10 ng of total cDNA was performed with the following primers: DGKδ, 5′-GTGGTGATCTCATCAGCC-3′ (forward) and 5′-TCTTCTCAGATTCAGAGAGG-3′; EGFR, 5′-GGAGGAAAAGAAAGTCTGCC-3′ (forward) and 5′-ATCGCACAGCACCAATCAGG-3′; TGFα, 5′-GTATCCTGTTAGCTGTGTGC-3′ (forward) and 5′-GCTTCTCATGTCTGCAGACG-3′; HB-EGF, 5′-GATGCTGAAGCTCTTTCTGG-3′ (forward) and 3′-GATGACAAGAAGACAGACGG-3′; amphiregulin, 5′-TTAGGCTCAGGCCATTATGC-3′ (forward) and 5′-ATCTGCATTCGCCATGAATGC-3′; tubulin, 5′-CAAGAACAGCAGCTACTTCG (forward) and 5′-CTGACAGAGGCAAACTGAGC-3′. Protocols and primer sets used to amplify mouse DGK isotypes are available on request.

Histological and *in Situ* Hybridization Analysis. Embryos and newborn mice were fixed in 10% neutral buffered formalin for 30–48 h, paraffin-embedded, sectioned (5 μm), and stained with hematoxylin/eosin according to standard protocol. Mouse DGKδ riboprobes (nucleotides 3451–4007 in human DGKδ cDNA from GenBank accession no. D73409) were made by using a DIG RNA Labeling Kit (Roche Molecular Biochemicals). This antisense probe showed only one band (6.7 kb) of mouse DGKδ mRNA by Northern blotting. *In situ* hybridization was performed as described in ref. 38. Immunostaining was performed by using ABC reagent (Vector Laboratories, Burlingame, CA) and anti-phospho-Thr-X-Arg (no. 2351) or anti-EGFR (no. 2232) from Cell Signaling Technonlogy (Boston, MA) or anti-keratin 6 (no. MK6, Covance, Cumberland, VA) according to instructions provided by the supplier.

Expression Plasmids, Cell Culture, and Transfection. Full-length human WT or T654A EGFR was cloned into pcDNA3.1/Myc-His (Invitrogen), and human DGKδ1 and DGKδ2 were cloned into p3XFLAG (Sigma, St. Louis, MO). Human PKCs α, δ, ε, and η were cloned into pCMV-myc (Clontech). Human pro-TGFα, pro-HB-EGF, proamphiregulin, and probetacellulin were cloned into pcDNA3.1/Zeocin. Primary mouse embryo fibroblasts were prepared from embryonic day 14.5 (8) and were grown in DMEM with 10% FBS and antibiotics. They were immortalized by transfection with simian virus 40 large T antigen (cloned into pcDNA3.1/Zeocin), followed by isolation of polyclonal populations of cells by selection with 100 μg/ml Zeocin (Invitrogen). Primary keratinocytes and dermal fibroblasts were isolated from newborn mice by overnight dispase II (Invitrogen) digestion. Keratinocytes were grown in Epilife medium with human keratinocyte growth supplement (Cascade Biologics, Portland, OR), and dermal fibroblasts were grown in DMEM with 10% FBS. MCF-7 cells were cultured in DMEM with 10% FBS and antibiotics. Transfection of expression vectors was performed by using Lipofectamine (Invitrogen) according to the manufacturer's instructions. Before treating cells with agonist (recombinant activin B no. 659-AB or TGFα no. 239-A, R & D Systems, Minneapolis, MN), all cells were starved for 24 h. DGKδ RNAi was performed by using Lipofectamine Plus (Invitrogen) and the siRNA duplex: 5′-GGC CAU GGU UCA CAC AUC GTT-3′ and 5′-CGA UGU GUG AAC CAU GGC CTT-3′. The dynamin II siRNA duplex is described in ref. 39. Scrambled siRNA duplexes were used as controls.

Western Blotting and Immunoprecipitation. Western blotting was performed according to instructions provided by the suppliers. The following antibodies were from Cell Signaling Technology: anti-phospho-Thr-X-Arg (no. 2351), anti-EGFR (no. 2232), anti-phospho-EGFR (no. 2234), anti-phospho-MARCKS (no. 2741), anti-phospho-JNK (no. 9251), and anti-phospho-cnPKC (no. 9371). Anti-MARCKS (sc-6454) and anti-PKCδ (sc937) were from Santa Cruz Biotechnology (Santa Cruz, CA). Anti-phospho-PKCα (no. 06-822) was from Upstate Biotech (Charlottesville, VA). Anti-FLAG M2 was from Sigma; anti-DGKδ is described in ref. 36. To quantify bands, scanned Western blot images were analyzed by using NIH ImageJ. Means and SD were calculated, and statistical significance was established by using paired, one-tailed *t* tests.

To test coimmunoprecipitation of DGKδ and PKC, cDNAs were transfected into MCF-7 cells. Forty-eight hours later, the cells were collected in lysis buffer (no. 9803; Cell Signaling Technology) and centrifuged to remove debris. The lysates (200 μg of protein) were incubated with anti-Myc overnight (at 4°C), and then protein A/G plus agarose (25 μl; Santa Cruz Biotechnology) was added for 1 h. After three washes with lysis buffer, the pellets and lysates (10 μg) were separated by SDS/PAGE and then immunoblotted to detect the DGK (anti-FLAG) or the

PKCs (anti-Myc). To immunoprecipitate transfected EGFR, we incubated 250 μg of cell lysate overnight at 4°C with anti-EGFR (Ab-13; Neomarkers, Fremont, CA) and added protein A/G plus agarose for 1 h, followed by washes as above. To immunoprecipitate endogenous EGFR, 2 mg of newborn liver or brain lysates was combined with anti-EGFR (no. E12020; Transduction Laboratories, San Jose, CA) overnight at 4°C; then, protein A/G agarose was added for 1 h, followed by washes as above.

DAG Quantity Assays. Immortalized embryo fibroblasts were starved overnight and treated with TGFα (10 ng/ml) for 15 min. Cells were washed once with PBS and harvested in methanol. Lipid extractions, DAG quantity assays, and lipid phosphate assays were performed as described in ref. 40.

Assays of TACE Activity. Primary or immortalized embryo fibroblasts were transfected with either control vector or a growth factor (TGFα, HB-EGF, amphiregulin, or betacellulin). Twenty-four hours later, the cells were starved overnight. Agonist (50 ng/ml phorbol ester, 2 units/ml thrombin, or 25 μM lysophosphatidic acid) in fresh medium was added for 30, 60, or 120 min. The medium was collected, and debris was pelleted. The amount of growth factor in the medium and cell lysates was then determined by using sandwich ELISAs (protocols are available on request). All agonists that were tested caused a 2- to 3-fold increase in growth factor shedding compared with nontreated controls. Results were normalized to total protein or growth factor in the lysate. Additional experiments testing the effects of overexpressing either DGKδ splice variant in HEK293, HeLa, or MCF-7 cells demonstrated no difference in growth factor release. To assay TNFα or p75 TNF receptor (TNFR) shedding, livers from newborn mice were homogenized in DMEM, and debris was allowed to settle. The remaining cell suspension (500,000 cells in 1 ml) was treated with agonist (5 μg/ml lipopolysaccharide or 50 ng/ml phorbol ester) for 3 h at 37°C. TNFα (no. KMC3012; Biosource, Carlsbad, CA) or p75 TNFR (no. 269SKI; PharMingen, San Jose, CA) was assayed in the cell lysate or medium by using sandwich ELISAs.

We thank Katrina Lund, Ethan Reichert, and Kelley Murphy for technical support; the transgenic/knockout mouse core facility at University of Utah; and Diana Stafforini for essential insight. This work was supported by National Institutes of Health Grant CA95463 (to M.K.T.), a grant from the R. Harold Burton Foundation (to M.K.T.), fellowships from the Mochida Memorial Foundation for Medical and Pharmaceutical Research and the Yamanouchi Foundation for Research on Metabolic Disorders (to F.S.), a fellowship from the Uehara Memorial Foundation (to A.T.), and National Cancer Institute Grant CA42014 (to the core facilities of University of Utah).

1. Topham MK (2006) *J Cell Biochem* 97:474–484.
2. van Blitterswijk WJ, Houssa B (2000) *Cell Signalling* 12:595–605.
3. Ron D, Kazanietz MG (1999) *FASEB J* 13:1658–1676.
4. Lucas P, Ukhanov K, Leinders-Zufall T, Zufall F (2003) *Neuron* 40:551–561.
5. Sakane F, Kanoh H (1997) *Int J Biochem Cell Biol* 29:1139–1143.
6. Imai H, Kai M, Yasuda S, Kanoh H, Sakane F (2005) *J Biol Chem* 280:39870–39881.
7. Rodriquez de Turco EB, Tang W, Topham MK, Sakane F, Marcheselli VL, Chen C, Taketomi A, Prescott SM, Bazan NG (2001) *Proc Natl Acad Sci USA* 98:4740–4745.
8. Regier DS, Higbee J, Lund KM, Sakane F, Prescott SM, Topham MK (2005) *Proc Natl Acad Sci USA* 102:7595–7600.
9. Zhong X, Hainey EA, Olenchock BA, Jordan MS, Maltzman JS, Nichols KE, Shen H, Koretzky GA (2003) *Nat Immunol* 4:882–890.
10. Li G, Gustafson-Brown C, Hanks SK, Nason K, Arbeit JM, Pogliano K, Wisdom RM, Johnson RS (2003) *Dev Cell* 4:865–877.
11. Zenz R, Scheuch H, Martin P, Frank C, Eferl R, Kenner L, Sibilia M, Wagner EF (2003) *Dev Cell* 4:879–889.
12. Weston CR, Wong A, Hall JP, Goad ME, Flavell RA, Davis RJ (2004) *Proc Natl Acad Sci USA* 101:14114–14119.
13. Yujiri T, Ware M, Widmann C, Oyer R, Russell D, Chan E, Zaitsu Y, Clarke P, Tyler K, Oka Y, *et al.* (2000) *Proc Natl Acad Sci USA* 97:7272–7277.
14. Peschon JJ, Slack JL, Reddy P, Stocking KL, Sunnarborg SW, Black RA (1998) *Science* 282:1281–1284.
15. Miettinen PJ, Berger JE, Meneses J, Phung Y, Pedersen RA, Werb Z, Derynck R (1995) *Nature* 376:337–341.
16. Sibilia M, Wagner EF (1995) *Science* 269:234–238.
17. Sahin U, Weskamp G, Kelly K, Zhou H-M, Higashiyama S, Peschon J, Hartmann D, Saftig P, Blobel CP (2004) *J Cell Biol* 164:769–779.
18. Hunter T, Ling N, Cooper JA (1984) *Nature* 311:480–483.
19. Davis RJ, Czech MP (1985) *Proc Natl Acad Sci USA* 82:1974–1978.
20. Cochet C, Gill GN, Meisenhelder J, Cooper JA, Hunter T (1984) *J Biol Chem* 259:2553–2558.
21. Baguinot L, Hanover JA, Ito S, Richert ND, Willingham MC, Pastan I (1985) *Proc Natl Acad Sci USA* 82:2774–2778.
22. Lin CR, Chen WS, Lazar CS, Carpenter CD, Gill GN, Evans RM, Rosenfeld MG (1986) *Cell* 44:839–848.
23. Lund KA, Lazar CS, Chen WS, Walsh BJ, Welsh JB, Herbst JJ, Walton GM, Rosenfeld MG, Gill GN, Wiley HS (1990) *J Biol Chem* 265:20517–20523.
24. Bao J, Alroy I, Waterman H, Schijter ED, Brodie C, Guruenberg J, Yarden Y (2000) *J Biol Chem* 275:26178–26186.
25. Seedorf K, Shearman M, Ullrich A (1995) *J Biol Chem* 270:18953–18960.
26. Luo B, Prescott SM, Topham MK (2003) *J Cell Biol* 160:929–937.
27. Arimoto T, Takeishi Y, Takeishi H, Shishido T, Niizeki T, Koyama Y, Shiga R, Nozaki N, Nakajima O, Nishimaru K, *et al.* (2006) *Circulation* 113:60–66.
28. Ueyama T, Lennartz MR, Noda Y, Kobayashi T, Shirai Y, Rikitake K, Yamasaki T, Hayashi S, Sakai N, Seguchi H, *et al.* (2004) *J Immunol* 173:4582–4589.
29. Aballay A, Stahl PD, Mayorga LS (1999) *J Cell Sci* 112:2549–2557.
30. Le TL, Joseph SR, Yap AS, Stow JL (2002) *Am J Physiol* 283:C489–C499.
31. Robinson PJ, Sontag JM, Liu JP, Fykse EM, Slaughter C, McMahon H, Sudhof TC (1993) *Nature* 365:163–166.
32. Topham MK, Prescott SM (2001) *J Cell Biol* 152:1135–1143.
33. Jones DR, Sanjuan MA, Stone JC, Merida I (2002) *FASEB J* 16:595–597.
34. Takahashi K, Yan B, Yamanishi K, Imamura S, Coulombe PA (1998) *Genomics* 53:170–183.
35. Colon-Gonzalez F, Kazanietz MG (2006) *Biochim Biophys Acta* 1761:827–837.
36. Sakane F, Imai SI, Kai M, Wada I, Kanoh H (1996) *J Biol Chem* 271:8394–8401.
37. Ding L, Traer E, McIntyre TM, Zimmerman GA, Prescott SM (1998) *J Biol Chem* 273:32746–32752.
38. Ding L, McIntyre TM, Zimmerman GA, Prescott SM (1998) *FEBS Lett* 429:109–114.
39. Huang F, Khvorova A, Marshall W, Sorkin A (2003) *J Biol Chem* 279:16657–16661.
40. Topham MK, Bunting M, Zimmerman GA, McIntyre TM, Blackshear PJ, Prescott SM (1998) *Nature* 394:697–700.